HORST SCHULTE

ADVANCED CONTROL OF GRID-INTEGRATED RENEWABLE ENERGY POWER PLANTS

LMI-BASED DESIGN IN THE TAKAGI-SUGENO FRAMEWORK

IEEEPress

WILEY

Advanced Control of Grid-Integrated Renewable Energy Power Plants

Advanced Control of Grid-Integrated Renewable Energy Power Plants

LMI-based Design in the Takagi-Sugeno Framework

Horst Schulte
Head of Control Engineering Group
HTW Berlin, Germany

WILEY

IEEE*Press*

This edition first published 2024

Registered Offices
John Wiley & Sons, Inc., 111 River Street, Hoboken, NJ 07030, USA
John Wiley & Sons Ltd, The Atrium, Southern Gate, Chichester, West Sussex, PO19 8SQ, UK

For details of our global editorial offices, customer services, and more information about Wiley products visit us at www.wiley.com.

Wiley also publishes its books in a variety of electronic formats and by print-on-demand. Some content that appears in standard print versions of this book may not be available in other formats.

Library of Congress Cataloging-in-Publication Data:

Names: Schulte, Horst, author.
Title: Advanced control of grid-integrated renewable energy power plants : LMI-based design in the Takagi-Sugeno framework / Horst Schulte.
Description: Hoboken, NJ : Wiley, 2024. | Includes bibliographical references and index.
Identifiers: LCCN 2024017996 (print) | LCCN 2024017997 (ebook) | ISBN 9781119701392 (hardback) | ISBN 9781119701408 (adobe pdf) | ISBN 9781119701286 (epub)
Subjects: LCSH: Power-plants. | Renewable energy sources. | Automatic control. | Convex functions.
Classification: LCC TJ164 .S345 2024 (print) | LCC TJ164 (ebook) | DDC 621.042–dc23/eng/20240517
LC record available at https://lccn.loc.gov/2024017996
LC ebook record available at https://lccn.loc.gov/2024017997

Cover Design: Wiley
Cover Image: © zhihao/Getty Images

Set in 9.5/12.5pt STIXTwoText by Straive, Chennai, India

Contents

Preface

Over the past 20 years, there has been a considerable growth in the installation capacity of renewable energy sources (RES) in power systems all over the world [IRENA, 2020]. In contrast to conventional power plants such as coal-fired or nuclear power plants with large synchronous machines, power plants with RES are much smaller and integrated into the grid via power electronic (PE) interfaces. This leads to a highly distributed structure and heterogeneous integration across all voltage levels into the power grid.

Currently, most renewable energy (RE) systems feed as much power as possible into the grid, but provide little or no grid support (i.e. ancillary services). In the future, this will no longer be sufficient to stabilize the grid due to the decreasing share of synchronous machine-based units. However, it is clear that the decentralized regenerative generators must be able to adapt the power quickly to the demand for frequency and voltage regulation via a suitable mix of grid-following and grid-forming converters, even without or less additional costs arising from battery energy storage systems (BESS) and as few additional control units as possible, such as FACTS and STATCOMS.

There is, still today, no common road map on how to systematically address this problem of grid operation with power-electronically coupled RES in practice. The book aims to contribute to this scientific question using methods of physical modeling, mathematical systems theory, and control engineering. Emphasis is on the development of model-based control concepts for photovoltaic and wind power plants, which are also intended to provide auxiliary services for grid frequency and voltage stabilization.

This book is useful for readers who want to gain knowledge of wind and photovoltaic (PV) power plant modeling and control with a deep understanding of model-based control concepts for optimal resp. flexible energy conversion and grid integration by inverters with grid-following and grid-forming operation. It is suitable for students from the fifth semester onward, experts from industry and academics, and PhD students who want to get an overview and possible

ideas on an exciting research topic. The intention was to provide a book with well-understandable description of the design models, the controller functions, and their validation presented in a unified control theory framework. The model and controller validation is done with high fidelity models (used for wind turbine control) or scenarios with measurement uncertainties (considered for PV systems).

This book is based on the results of research projects I have worked on and mostly managed over the past 10 years. The aim was to make the results available to the community in a closed and understandable form, for both professionals and graduate students working on control systems or electrical power systems. I thank my wonderful colleagues and collaborators Prof. S. M. Esmailifar, Prof. J. Fortmann, E. Gauterin, Dr. S. Goerg, N. Goldschmidt, Prof. N. Klaes, Dr. S. Kusche, Dr. Z. R. Labidi, and Dr. F. Pöschke for the many valuable discussions and exchanges without which this book would not have taken the form it has.

Berlin *Horst Schulte*
September 2023

Acronyms

AC	alternating current
AGC	automatic generation control
APC	active power control
AS	ancillary services
AVR	automatic voltage regulator
BMI	bilinear matrix inequality
CIG	converter-interfaced generation
DC	direct current
DER	distributed energy resource
DFIG	doubly fed induction generator
DOF	degree of freedom
DPT	demanded power tracking
DSO	distribution system operator
DVPP	dynamic virtual power plant
EMT	electromagnetic transient
EPS	electrical power systems
ESC	extremum-seeking control
FACTS	flexible alternating current transmission system
FAST	Fatigue, Aerodynamics, Structures, and Turbulence model
FLL	frequency-locked loop
HAWT	horizontal-axis wind turbine
HC	hill climbing
HIL	hardware in the loop
HPP	hybrid power plant
HV	high voltage
HVDC	high-voltage direct current
IBR	inverter-based resource
iff	if and only if
IGBT	insulated-gate bipolar transistor

IOS	input-to-output stability
ISS	input-to-state stability
LDI	linear differential inclusion
LHS	left-hand side
LIDAR	light detection and ranging
LMI	linear matrix inequality
LQR	linear quadratic regulator
LPV	linear parameter variable
LTI	linear time invariant
MATLAB®	Matrix Laboratory
MPP	maximum power point
MPPT	maximum power point tracking
MIMO	multiple-input multiple-output
NREL	National Renewable Energy Laboratory
PE	power electronic
PCC	point of common coupling
PDC	parallel distributed compensation
PLL	phase-locked loop
PMSG	permanent magnet synchronous generator
P&O	perturbation and observation
PI	proportional-integral
pu	per unit
PV	photovoltaics
RPP	renewable energy power plant
RES	renewable energy source
RHS	right-hand side
RMS	root mean square
SISO	single-input single output
SL	sector-nonlinearity (approach)
STATCOM	static synchronous compensator
s.t.	such that
STC	standard test condition
TS	Takagi-Sugeno
TSO	transmission system operator
VPP	virtual power plant
VSC	voltage-sourced converters
WPP	wind power plant
WT	wind turbine
WTG	wind turbine generator

Notation

- Italic denotes scalar physical quantities (e.g. R, L, and C) or numerical variables (e.g. x and y).
- Italic boldface denotes a matrix (capital letters) or a vector (small letters), e.g. $\mathbf{A}, \mathbf{B}, \mathbf{x}$, and $\mathbf{y}$.
- Unit symbols are written using roman type (e.g. Hz, A, and kV).
- Standard mathematical functions are written using roman type (e.g. e, sin, cos, and arctan).
- Lowercase symbols normally denote instantaneous values (e.g. v and i).
- Uppercase symbols normally denote RMS or peak values (e.g. V and I), exception: active and reactive power denoted as P and Q.
- Subscripts d and q refer to the direct- and quadrature-axis components.
- Subscripts α and β refer to α and β components of a three phase system.
- Italic underline type denotes a phasor (e.g. $\underline{I}, \underline{V}$, and $\underline{S}$).
- Lowercase symbol with upper arrow denotes a space vector $\vec{\mathbf{x}}$.

1

Introduction

1.1 Energy Transition

Public discussion about the energy transition is dominated by the need to accelerate the planning and installation of wind farms and photovoltaic (PV) plants, as well as the grid expansion by new lines and deferrable loads. That is obvious and quite understandable. Far less known and not a subject of public debate is that the transition to renewable energy also means that the traditional use of synchronous machines, which still regulate frequency and voltage in the grid [Machowski et al., 2008], is being replaced by power electronic (PE)–based converter-interfaced renewable energy sources (RES). The transition to a massive integration of PE-based power plants [Peng et al., 2018a], also called inverter-based (IBG) [Joi, 2018] or converter-interfaced generators (CIG), which began in the decade of the new millennium, enables relatively flexible and efficient power conversion. Such a transition implies all areas within power systems and may be considered a paradigm shift in the sense of Kuhn [1962]. Because power systems fundamentally change in power generation, transmission, and distribution, this has significant implications for the associated engineering and scientific disciplines, as questions of stability, control, and reliability must be addressed in new ways.[1]

Symptomatic of the fundamental change in power systems is the distributed generation by many heterogeneous units feeding power to different grid levels by power electronic interfaces. At the transmission level, for example, offshore wind farms feed in, at the sub-transmission level the onshore wind farms or large PV power plants are integrated, and at the distribution level medium-sized PV power plants. Instead of generators connected to the grid via stator windings, rotating units in renewable energy systems are decoupled from the grid: these cannot

1 Operation and control, stability analysis, computational methods of power systems, protection and automation, power electronics, active distribution systems, and distributed energy resources. The disciplines were chosen partly to follow the names of CIGRE's study committees and their work areas.

Advanced Control of Grid-Integrated Renewable Energy Power Plants: LMI-based Design in the Takagi-Sugeno Framework, First Edition. Horst Schulte.

contribute to system inertia without additional active control. Until now, the frequency and voltage stability characteristics of power systems have been strongly determined by large synchronous generators driven by steam or gas turbines.

Let us first consider the frequency dynamics in conventional power systems. Assuming a common frequency in the AC network,[2] the instantaneous rate of change of frequency (RoCoF) after the disconnection of a generator (generator tripping) or load from a power system before any control becomes active can be computed as follows [ENTSO-E, 2018]

$$\frac{d\Delta f}{dt} = \frac{f_0\,\Delta P}{2\sum_{i=1}^{N_g} H_i\,S_{n,i}}\,, \qquad \Delta f = f - f_0, \tag{1.1}$$

with $d\Delta f/dt$ as derivative of the difference frequency f related to the nominal system value f_0, where H_i is the inertia constant

$$H_i = \frac{E_{k,i}}{S_{n,i}} = \frac{J_i\,\omega_{sm}^2}{2}\,\frac{1}{S_{n,i}}, \tag{1.2}$$

of each generator $i = 1, \ldots, N_g$, where $E_{k,i}$ is the kinetic energy of the generator running at synchronous (nominal) speed $\omega_{sm,i}$. Each turbine's total moment of inertia plus the generator rotor is denoted as J_i. The variable $S_{n,i}$ is the rated apparent power of each generator. Here, the inertia constant H_i describes the property of the synchronous machine i to maintain the system state of uniform rotary motion when no external torque is applied. A typical value of H for a synchronous generator can range from two to nine seconds. The active power deviation ΔP in (1.1) is defined by the summation of all mechanical shaft power input to the generator units $P_{m,i}$ for $i = 1, \ldots, N_g$ and the electrical air-gap power $P_{e,i}(\delta_i)$ caused by system loads in the grid and controlled by the power angle or load angle δ, both expressed in watts

$$\Delta P = \sum_{i=1}^{N_g} \left(P_{m,i} - P_{e,i}(\delta_i)\right), \tag{1.3}$$

where N_g denotes the total number of generator units. For the interpretation of (1.1) it must be noted that RoCoF is triggered by unplanned load shedding or generator tripping. In case of generator tripping k (i.e. $P_{m,k} \to 0$) the remaining generators ($\forall i \neq k$) provide a frequency change inversely proportional to $\sum_{i=1,i\neq k}^{N_g} H_i\,S_{n,i}$. This behavior results from the swing equation of each generator represented by two first-order equations [Machowski et al., 2008]

$$\begin{aligned} \frac{2H_iS_{n,i}}{\omega_s}\,\Delta\dot{\omega}_i &= -d_m\,\Delta\omega_i + P_{m,i} - P_{e,i}(\delta_i), \\ \dot{\delta}_i &= \Delta\omega_i + \omega_s, \end{aligned} \tag{1.4}$$

2 The effects of local frequency variations in power systems during transition as deviations from the global nominal frequency, and their modeling and estimation, are studied, i.e. in Milano and Manjavacas [2020].

with $\Delta\omega_i = \omega_i - \omega_s$, where ω_i denotes the electrical rotor speed, $\omega_s = 2\pi f_o$ denotes the electrical synchronous speed resp. synchronous angular frequency, δ_i denotes the power angle, and d_m is the damping coefficient. Introducing an aggregated[3] rotor speed $\Delta\omega_i \approx \Delta\omega$ and $\Delta\dot{\omega} = 2\pi\Delta\dot{f} \approx \Delta\dot{\omega}_i$ in (1.4), and after summation

$$\frac{2\sum_{i=1}^{N_g} H_i S_{n,i}}{f_o}\,\Delta\dot{f} = -\sum_{i=1}^{N_g} d_m\,\Delta\omega + \sum_{i=1}^{N_g}\left(P_{m,i} - P_{e,i}(\delta_i)\right), \tag{1.5}$$

and by neglecting the damping term, we obtain the RoCoF index (1.1). It is evident that the RoCoF value increases caused by a decrease of $\sum_{i=1}^{N_g} H_i S_{n,i}$ due to the substitution of synchronous generators by inertia-less (PV power plants) or inertia-decoupled (wind turbines[4]) generator units. In summary, the energy transition with a high penetration of CIGs with over 80% and more in the future has the effect that the RoCoF value of electrical power systems (EPS) significantly increases which leads to a stronger fluctuation of the grid frequency and an increase of the probability of frequency instability.

In addition to frequency regulation, the voltage control of grids with a high percentage of PE-based converter-interfaced generators must also be addressed. In contrast to grid frequency, which can be modeled as a global quantity, the voltage in power grids has to be considered as a local quantity, which can vary strongly in the permitted bounds from node to node. The voltage level could be changing due to factors related to generation, transmission, and distribution. However, the variability of the load is one of the most important factors. The voltage must remain within a specified range because over-voltage implies an increase in active power losses and, as a long-term effect, can increase the probability of insulation failure. Thus control is needed to maintain the grid voltage in a permissible range, and if a short circuit occurs, it must be ensured that voltage drops are limited.

In AC networks with typically overhead transmission line parameters $X \gg R$ (see [Kundur, 1994], Table 6.1) the voltage states are strongly coupled with the reactive power fluxes. For example, the longitudinal voltage drops in the networks are caused by the reactive power currents. For the line element shown in Figure 1.1, the reactive power flow Q of a single-phase system[5] is given by

$$Q = \frac{EV}{X}\cos\delta - \frac{V^2}{X}, \tag{1.6}$$

3 i.e. Based on the center of inertia (COI) frequency ω_{COI} [Kundur, 1994].

4 Note, this is also the case for wind turbines with doubly fed induction generator (DFIG). Although the generator stator is directly connected to the grid, the inverter-based variable frequency excitation in the rotor decouples the speed of the turbine rotor speed from the grid frequency.

5 A balanced three-phase has three times the power of a single-phase system. The more general case with a resistor R and reactance $X = \omega L$ as line impedance is calculated in Chapter 5, with the result (5.58).

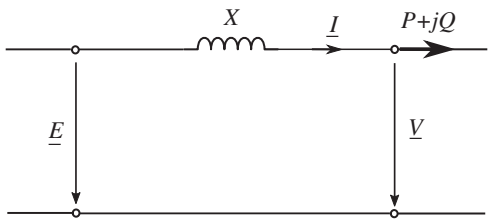

Figure 1.1 Single-phase equivalent circuit of a line with $X = \omega L$

with the impedance $X = \omega L$, where δ denotes the angle between the voltage phasor of the generator resp. converter $\underline{E}$ and $\underline{V}$ at the reference point to the right of the line inductance

$$\underline{E} = E\, e^{j0}, \qquad \underline{V} = V\, e^{j\delta}, \tag{1.7}$$

with the root mean square (RMS) voltage values E and V. The associated active power of a line element of a single-phase system is determined by

$$P(\delta) = \frac{EV}{X} \sin \delta. \tag{1.8}$$

It can be seen that the active power P depends on the product of phase voltages and the sine of the angle δ between their phasors. Because in power systems the node voltages are only within a small percentage of their nominal values, the large changes in active power result from the power angle δ [Machowski et al., 2008]. Note that with the power relations (1.6), (1.8), and the swing equation (1.4) power dynamics of networks with one, two, and multiple generators can be studied in the control loop and under consideration of power plant interactions. In Chapters 5 and 6 such investigations are presented after model-based control concepts of renewable energy (RE) generation (wind and solar) were presented and discussed in Chapters 2–4.

In summary, for reliable power system operation, the provision of ancillary services (AS) will have to be provided to a large extent by renewable energy systems in the future. A possible transformation of how AS will be provided in the future is shown in Figure 1.2 from Komarnicki et al. [2023]. In this process, AS from large synchronous generators are first provided by flexible alternating current transmission system (FACTS), STATCOMS, and high-voltage direct current (HVDC), which are increasingly being replaced by massive distributed inverter-coupled RE generation up to half. Since these are primarily installed in the distribution grid, it will be a significant challenge to make those AS from the distribution also available to the transmission grid. Note that Figure 1.2 from Komarnicki et al. [2023] also includes system recovery and system control services, such as black start capability [DENA, 2014], which are not addressed in this study. The focus of this book is, that in addition to the important regular feed-in control operation, that wind

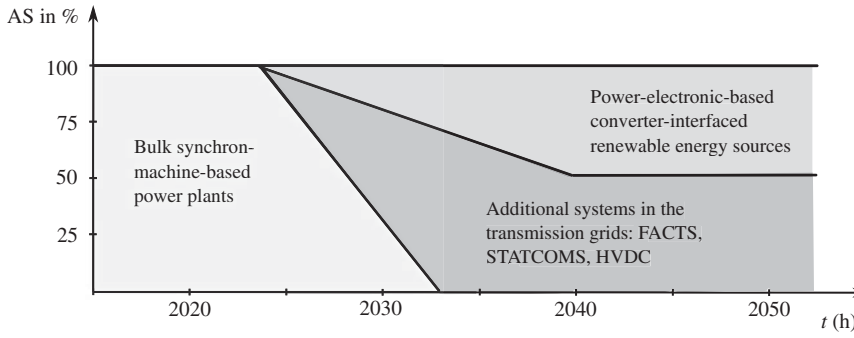

Figure 1.2 Which technology will provide ancillary grid services in the future?

and PV power plants are able to provide flexible services for frequency regulation, such as instantaneous reserve, primary frequency control, and voltage regulation. As shown in Figure 1.2, a share of at least 50% and possibly more should be reliably achieved from 2040. A detailed formal problem description of how wind power and solar PV power plants are able to provide AS is given in Section 1.2.

1.2 Problem Description

Renewable energy systems, such as wind and photovoltaic systems, should either feed as much power as possible into the grid or, if needed but also available, follow a requested power demand. It should be considered that the maximum power that can be fed into the grid obviously depends on the currently available power if no additional storage is used. The power plants are connected to the grid via electronic-based converters and power transformers. The latter is needed to increase the converter's low-voltage level to the grid's medium-voltage level, i.e. between 10 and 35 kV. The grid-side converter is connected to the primary winding of the transformer with an LCL filter. The reference power is generated locally or by an external higher-level controller.

The generic structure of a generation unit to be considered is illustrated in Figure 1.3. The scheme shows the relationships of both wind and photovoltaic (PV) power plants concerning the power flow, measurements, and control signals. Here, the regenerative energy resource as the wind flow in the rotor disc or the irradiation per area is converted into the electrical power P_g of the wind turbine generator or the aggregated DC power P_{dc} of a solar power plant. The wind turbine (WT) generator and PV array, also called PV generator, feed power into the DC link, which is assigned to the "secondary power conversion" block. The secondary

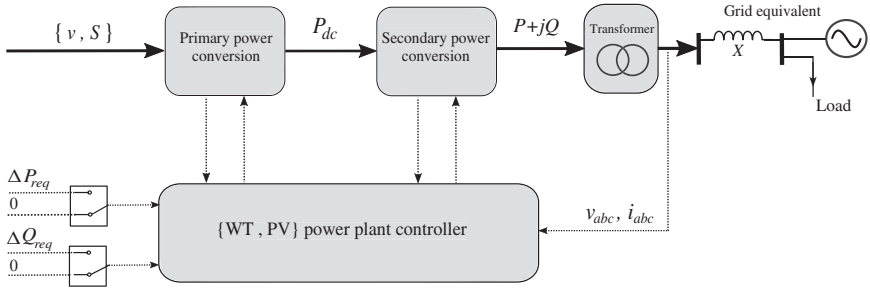

Figure 1.3 Functional diagram of grid-integrated renewable power plant with primary, secondary power conversion, control system, and external reference signals

block contains a voltage-source converter (VSC) that generates a three-phase AC system from the DC link voltage by a suitable switching logic. For this purpose, the standard space vector modulation (SVM) is applied. In combination with an LCL filter to reduce the current harmonics caused by switching, power is fed into the grid.

The two subsystems, the primary and secondary power conversion, are automatically regulated where the controller of the primary conversion subsystem aims to regulate the internal states (rotor speed ω_r or PV voltage v_{pv}) in relation to the states of external resources. The control objective is to either extract the maximum possible power from the renewable resource or to follow a reference power signal, taking into account the achievable limits of the resource. The desired behavior is represented by two modes: (a) generation of the maximum possible electrical power and (b) follow, if possible, the power request ΔP_{req} and ΔQ_{req}.

To clarify the control task of the primary conversion in renewable energy systems, we will use the P–x curves. Solar PV power plants' primary conversion is characterized by the power–voltage curve (P–V curve) parameterized via the irradiation S as power per area in W/m^2. Similarly, for wind turbines, the production by the WT generator is given as power over rotor speed (P–ω_r curve) parameterized with the effective wind speed v in front of the rotor. In grid-feeding mode, the task of "primary converter control" is to feed as much power as possible into the grid. In addition, other tasks must be covered by the power plant controller in Figure 1.3. For example, the generated power of wind turbines at high wind speeds should not permanently exceed the rated power of the generator. Therefore, at or above the rated wind speed, the wind turbines are operated at a constant speed (rated speed) with constant torque (rated torque). To achieve this, the pitch angle of the rotor blades is regulated to reduce the rotor's torque and adapt it to the nominal torque of the generator. To provide flexible power control for AS, the strategies described above must be superimposed with a deloading procedure. For a formal

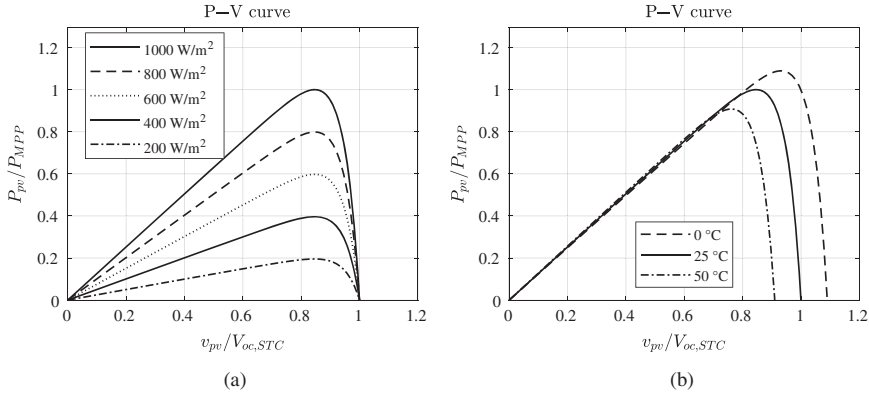

Figure 1.4 *P–V* curve of PV solar modules in pu with variation of irradiation S and cell temperature T_c. The power P_{pv} is related to the maximum power by standard test conditions (STC) and the voltage is related to the open-circuit voltage $v_{oc,STC}$ by STC

problem description of the control task of the primary conversion systems, some known characteristic curves for solar PV and wind turbines are now utilized.

First, to characterize the basic control problem of **wind turbines**, the power–rotor speed curve (P_r–ω_r curve) is shown in Figure 1.5. It can be noticed, the point of maximum power changes with varying wind speed. Therefore, to reach the point of maximum power with fluctuating wind speed, the rotor speed must be adjusted according to the P_r–ω_r curve. To achieve this, the rotor speed is changed by the generator torque. Depending on whether the generator torque at the low speed shaft is greater or less than the instantaneous rotor torque, the generator speed increases or decreases. Unless the generator torque reaches the nominal torque limit, the speed can be adjusted within the nominal speed range $\omega_{r,cut\text{-}in} \leq \omega_r \leq \omega_{r,rated}$ 1.2, where $\omega_{r,cut\text{-}in}$ denotes the cut-in and $\omega_{r,rated}$ the nominal rotor speed. If the rotor speed increases to the nominal speed due to the increasing wind speed, the control goal of maximum power tracking is left and the rotor speed is kept on the nominal speed using set point control by increasing generator torque. If the nominal generator torque is reached here as well, the increase in speed is controlled by adjusting the pitch angle of the rotor blades instead.

The scheme described so far is the conventional control scheme without active power control. Additional flexible power change for grid supporting can be achieved by a superimposed generator torque adjustment whereby the operating point related to the rotor torque is not left by adapting the rotor torque by means of pitch angle control. This means that the decoupling of the control problem into

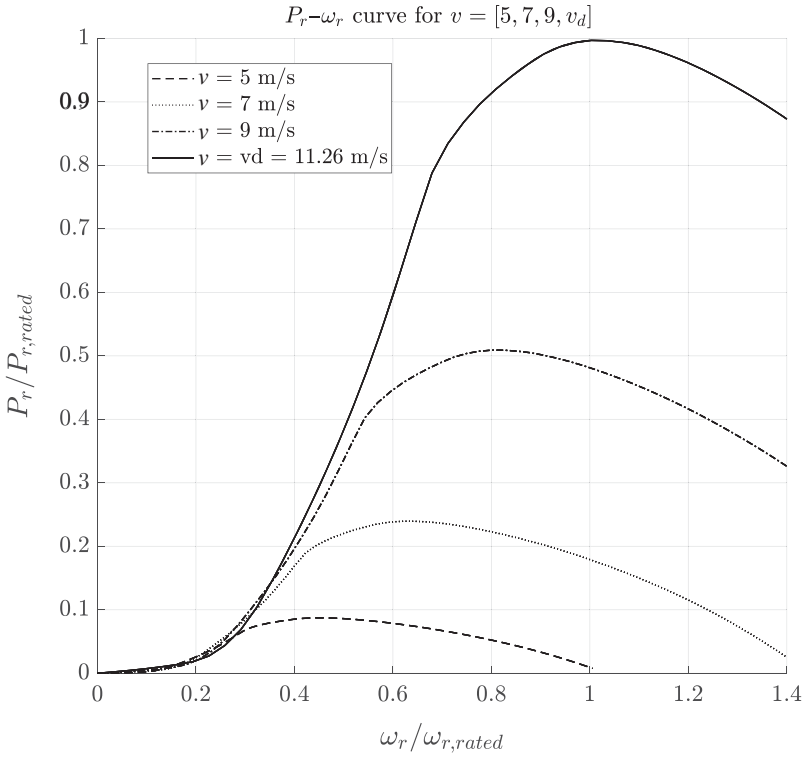

Figure 1.5 P_r–ω_r curve of wind turbines in pu for pitch angle $\beta = 0°$, where v_d denotes the design also called the rated wind speed v_{rated}. Further details are presented in Chapter 2

two single input single output (SISO) designs[6] can no longer be utilized. Instead, a multi-variable control method must be used. Indeed, the control system proposed in this book follows a rigorous model-based approach, where the controller design is performed by solving an optimization problem with linear matrix inequality (LMI) constraints. The modeling of wind turbines for the design is described in Chapter 2. The controller concepts for an optimal and flexible power control and model-based controller synthesis are presented in detail in Chapter 3.

Second, for **solar PV systems**, the essentials of power optimization will be described by the illustration in Figure 1.4. In power-feeding mode the control objective is to track the point of maximum power, also called maximum power point (MPP). Due to the change in radiation $S \in \{200, \ldots, 1000\}\text{W/m}^2$ and the cell temperature $T_c \in \{0, 25, 50\}\,°\text{C}$, see Figure 1.4, the MPP position in the

6 Single-input single-output with generator torque as plant input during partial-load region and the collective pitch-angle as plant input during full-load region with the rotor speed as a common system output.

$P-V$ curve changes. To track the MPP, the voltage v_{pv} is adjusted by a DC–DC converter. For AS, particularly grid support with negative regulating power, the solar PV generator must also be able to reduce the generated power as fast as possible. This is achieved by leaving the MPP. For positive regulating power, the plant can be permanently derated by 10% to 15%. As a result, this percentage is then available without additional storage to increase the generated power. To be seen in the $P-V$ curve of Figure 1.4, increasing or decreasing the voltage v_{pv} set by the DC-DC converter results in a flexible power adjustable output.

Both modeling the controller concepts and synthesis for MPP and flexible power control are presented in detail in Chapter 4.

In addition to the primary conversion presented in PV and wind power systems, the problem of **secondary conversion** is now described **for both systems** together. As shown in Figure 1.3, the secondary system with the DC power, denoted as P_{dc}, is supplied by the primary converter. In wind turbines (Type 4 WT), this is achieved by an AC–DC converter connected in series with the generator. In PV system, the DC power of PV generators, denoted as P_{pv}, is converted into P_{dc} by DC–DC circuits. The main component in the secondary converter block is the VSC. In recent years, a distinction has been made between grid-following (GFL) and grid-forming (GFM) converters, which, in combination with the appropriate primary converter control, determine the overall system behavior of a RE power plant. State-of-the-art control concept for a GFL converter and two concepts for a GFM converter are presented in detail.

1.3 Methodological Framework

The methodological framework in this book is based first on the use of Takagi–Sugeno (TS) models [Takagi and Sugeno, 1985] as a class of nonlinear state-space models, which are similar to linear parameter variable (LPV) models[7] and second the model-based control and observer synthesis formulated as an optimization problem with linear matrix inequality (LMI) constraints. An optimization problem with LMI constraints is usually called a semi-definite programming problem (SDP) which can be considered an essential tool in several branches of control theory and signal processing [Boyd et al., 1994]. The use of TS models for controller design in combination with LMI constraints was first described in the monograph [Tanaka and Wang, 2001]. Since then, the methods have been further developed and applied in areas where classical methods of nonlinear control are either not robust enough or have too many assumptions in the synthesis. To use

7 In Schulte and Pöschke [2016] the differences and similarities are explained using case studies for TS sliding observer-based fault diagnosis of an inverted pendulum and a wind turbine with horizontal axis. The formulation has in common the use of scheduling variables (called premise variables in the fuzzy context) and the weighted combination of LTI models with convex sums.

the TS framework for modeling dynamic systems, either a nonlinear state-space description is either derived from first principle equations or estimated from measured data by suitable system identification methods including model order selection. The latter data-based approach is still an unsolved problem in the general formulation. For certain classes of TS/LPV models, there are solutions which, in their restricted form, are not suitable for the problems dealt with in this book.

In the method applied here, we derive nonlinear state-space models from the first principles and cast them into a suitable TS formulation. The state-space model to be derived has the following form

$$\begin{aligned} \dot{\mathbf{x}} &= \mathbf{f}(\mathbf{x}, \mathbf{u}, \boldsymbol{\theta}), \qquad \mathbf{x}_0 = \mathbf{x}(t_0), \\ \mathbf{y} &= \mathbf{g}(\mathbf{x}), \end{aligned} \tag{1.9}$$

where $\mathbf{f} : \mathbb{R}^n \to \mathbb{R}^n$ and $\mathbf{g} : \mathbb{R}^n \to \mathbb{R}^p$ are smooth vector-valued functions, $\mathbf{x} \in \mathbb{R}^n$ denotes the state-space vector, $\mathbf{u} \in \mathbb{R}^m$ is the input vector with controllable and uncontrollable inputs, $\boldsymbol{\theta} \in \mathbb{R}^d$ denotes a time variable parameter vector, and $\mathbf{y} \in \mathbb{R}^p$ denotes the output vector. In this study the Takagi–Sugeno (TS) models are derived by the sector-nonlinearity approach [Ohtake et al., 2001] or by classical linearization at a set of equilibrium points and appropriate choice of functions $h_i : \mathbb{R}^l \to \mathbb{R}$ with values greater than zero in a local region around the related equilibrium point. In this work two different classes of TS models are used, first weighted combination of linear state-space models

$$\begin{aligned} \dot{\mathbf{x}} &= \sum_{i=1}^{N_r} h_i(\mathbf{z}) \, \left(\mathbf{A}_i \mathbf{x} + \mathbf{B}_i \mathbf{u} \right), \qquad \mathbf{x}_0 = \mathbf{x}(t_0), \\ \mathbf{y} &= \sum_{i=1}^{N_r} h_i(\mathbf{z}) \, \mathbf{C}_i \mathbf{x}, \end{aligned} \tag{1.10}$$

or affine state-space models

$$\begin{aligned} \dot{\mathbf{x}} &= \sum_{i=1}^{N_r} h_i(\mathbf{z}) \, \left(\mathbf{A}_i \mathbf{x} + \mathbf{B}_i \mathbf{u} + \mathbf{a}_i \right), \qquad \mathbf{x}_0 = \mathbf{x}(t_0), \\ \mathbf{y} &= \sum_{i=1}^{N_r} h_i(\mathbf{z}) \, \left(\mathbf{C}_i \mathbf{x} + \mathbf{c}_i \right), \end{aligned} \tag{1.11}$$

with $\mathbf{A}_i \in \mathbb{R}^{n \times n}$, $\mathbf{B}_i \in \mathbb{R}^{n \times m}$, $\mathbf{C}_i \in \mathbb{R}^{p \times n}$, $\mathbf{a}_i \in \mathbb{R}^n$, and $\mathbf{c}_i \in \mathbb{R}^p$. The functions $h_i : \mathbb{R}^l \to \mathbb{R}$ are denoted as membership functions and fulfill the convex sum condition

$$0 \le h_i(\mathbf{z}) \le 1, \quad i = 1, 2, \dots N_r, \qquad \sum_{i=1}^{N_r} h_i(\mathbf{z}) = 1 \quad \forall \mathbf{z}. \tag{1.12}$$

The vector of the so-called premise variables may directly contain states x_k, inputs u_k, and time variable parameters θ_k or be a function $\mathbf{z} = \mathbf{z}(\mathbf{x}, \mathbf{u}, \boldsymbol{\theta})$. The classic

notation of fuzzy rules with linguistic variables is replaced by the sum notation. It has become apparent that the fuzzification and defuzzification from the original work [Takagi and Sugeno, 1985] does not bring any advantages in the system analysis and controller synthesis. The validity of the linear models in the entire system is quantified by the membership function h_i. The name arises from the property that validity resp. membership of the linear or affine models in the overall model (1.10) or (1.11) is determined with h_i.

The steps necessary to construct TS models (1.10) and (1.11) based on (1.9) which are suitable for the controller and observer design are described in Chapter 2 "Modeling of Wind Turbines" and Chapter 4 "Modeling and Control of Photovoltaic Power Plants." It is worth mentioning that the choice of membership functions and sub-models is not unique. When applying the method with sector functions, it must be ensured that the observability and controllability of the linear submodels are preserved. Because, from the clustering of the nonlinearities of the original model (1.9) in the membership functions, it may occur that the structural coupling of the states and inputs in the linear submodels is partially or completely removed. How to solve this problem by a suitable formulation is described in Chapters 2 and 3.

The TS control laws used in this work contain the plant model membership function $h_i(\mathbf{z})$. In the literature, this structure is called a parallel distributed compensator (PDC) [Tanaka and Wang, 2001]. The PDC form used here is a generalization of the integral state feedback controller of linear time-invariant (LTI) systems [Franklin et al., 1994] to the case of nonlinear systems in Takagi–Sugeno form [Schulte and Hahn, 2004]:

$$\mathbf{u} = \sum_{i=1}^{N_r} h_i(\mathbf{z}, \hat{\mathbf{z}}) \left(-\mathbf{K}_{x,i}\, \mathbf{x} + \mathbf{K}_{I,i}\, \mathbf{x}_I \right), \quad \mathbf{x}_I = \int_0^t \left(\mathbf{y}_{ref}(\tau) - \mathbf{y}(\tau) \right) d\tau, \tag{1.13}$$

where $\mathbf{y}_{ref}$ denotes the reference signal. The state feedback gain $\mathbf{K}_x$ and the gain of integral action $\mathbf{K}_I$ are computed by optimization problems with LMI constraints involving the sub-models with $\{\mathbf{A}_i, \mathbf{B}_i, \mathbf{C}_i\}$ resp. $\{\mathbf{A}_i, \mathbf{B}_i, \mathbf{a}_i, \mathbf{C}_i, \mathbf{c}_i\}$ of (1.10) resp. (1.11) and the closed-loop reference dynamics in the form of convex parameterized pole regions (see Appendix B). We do not assume that all premise variables are measurable. Therefore, a distinction is made between measurable $\mathbf{z}$ and estimated $\hat{\mathbf{z}}$ premise variables. For example, a disturbance variable observer is used to estimate the effective wind speed in front of the turbine rotor [Gauterin et al., 2015]. The observer law for state and disturbance variable compensation used in this work reads in its general form

$$\begin{aligned} \dot{\hat{\mathbf{x}}} &= \sum_{i=1}^{N_r} h_i(\mathbf{z}, \hat{\mathbf{z}}) \left(\tilde{\mathbf{A}}_i\, \hat{\mathbf{x}} + \tilde{\mathbf{B}}_i\, \mathbf{u} + \mathbf{L}_i \left(\mathbf{y} - \hat{\mathbf{y}} \right) \right), \\ \hat{\mathbf{y}} &= \sum_{i=1}^{N_r} h_i(\mathbf{z}, \hat{\mathbf{z}})\, \tilde{\mathbf{C}}_i\, \hat{\mathbf{x}}, \qquad \hat{\mathbf{x}}_0 = \hat{\mathbf{x}}(t=0), \end{aligned} \tag{1.14}$$

with $\hat{\tilde{\mathbf{x}}} = (\hat{\mathbf{x}}^T, \hat{\mathbf{z}}^T)^T$, where $\mathbf{L}_i$ denotes the observer gain related to each i-th sub-model with $\{\mathbf{A}_i, \mathbf{B}_i, \mathbf{C}_i\}$. The augmented state vector contains the estimated system states $\hat{\mathbf{x}}$ of (1.10) and the disturbance, in this case the unmeasurable premise variables $\hat{\mathbf{z}}$. The observer (1.14) is a generalization of the Luenberger–Observer of LTI systems [Luenberger, 1964] to the case of nonlinear systems in Takagi–Sugeno form.

1.4 Topics of this Book

This book is helpful for readers who want to gain knowledge of mathematical modeling and modern control design of solar photovoltaic and wind power systems. Novel controller structures are presented that enable the RE power plants not only to feed the grid with energy but also to support the grid by fast frequency response and voltage control. The rigorous, model-based approach is presented to encourage readers to understand the paradigm shift in distributed renewable generation and to apply the resulting methods in system development.

The book is suitable for undergraduate and graduate levels with a control system or energy engineering background. In addition to graduate and PhD students, the book may serve as a helpful reference for academic researchers, engineers, and other professionals in the industry. Due to the strict model-based approach, readers with a control system background learn more about the physics and design of wind and solar photovoltaic power generation, including grid integration via power-electronic-based VSC. The control methods are both introduced and explained in the main text, and further technical details are given in the appendixes. This allows readers without a background in control theory to concentrate on the essentials, while others will find further references in the appendix. Most of the chapters contain an introduction to the topic with baseline concepts for modeling and control and advanced concepts to meet modern requirements for grid support. Pictures, illustrations of control schemes, and simulation results support the mathematical and analytical considerations. Furthermore, each chapter contains literature references and problems for self-study. The solutions are provided online.

The book contains six chapters: After the introduction in Chapter 1 the following Chapter 2 proposes mathematical models to describe an entire horizontal axis wind turbine from aerodynamics, structural dynamics, and the actuators for control purposes. The appropriate combination of subsystems results in different design models with varying levels of complexity to achieve applicable optimization criteria. Based on the control objectives for power fed-in and flexible power support for fast frequency control Chapter 3 presents related control schemes and LMI-based design methods in the Takagi–Sugeno